

## IN-SITU OBSERVATION OF STRESS-FIELD PROPAGATION AND DAMAGE FORMATION IN HYPERVELOCITY-IMPACTED GLASS MATERIALS

Nobuaki Kawai<sup>1</sup>, Tomo Uemura<sup>2</sup>, Kazuma Watanabe<sup>2</sup>, Sunao Hasegawa<sup>3</sup>

<sup>1</sup>National Defense Academy, Yokosuka, Japan

<sup>2</sup>Kumamoto University, Kumamoto, Japan

<sup>3</sup>Japan Aerospace Exploration Agency, Sagamihara, Japan

### ABSTRACT

*Hypervelocity impact experiments have been conducted on quartz glass and soda-lime glass to observe directly the impact-induced damage process progressing inside materials. Stress wave propagation and damage evolution associated with hypervelocity impact are visualized by employing the Edge-on Impact technique coupled with the polarized light shadowgraphy or scattered-light imaging method using an ultra-high-speed video camera. Recorded images clearly show how stress waves propagate and interact with each other, and how damages form and propagate during hypervelocity-impact events. A comparison of damage structures between quartz and soda-lime glasses reveals that differences in the short-range order of atomic configurations can affect the formation of macroscopic impact damage in amorphous materials such as glass. In experiments with a target consisting of two soda-lime glass components stacked in the direction of the ballistic axis, it is observed that damage form and propagate in the vicinity of the interface due to the interaction between the contact interface of the two glass components and the stress wave.*

Keywords: Hypervelocity impact, High-speed imaging, Glass, Impact damage

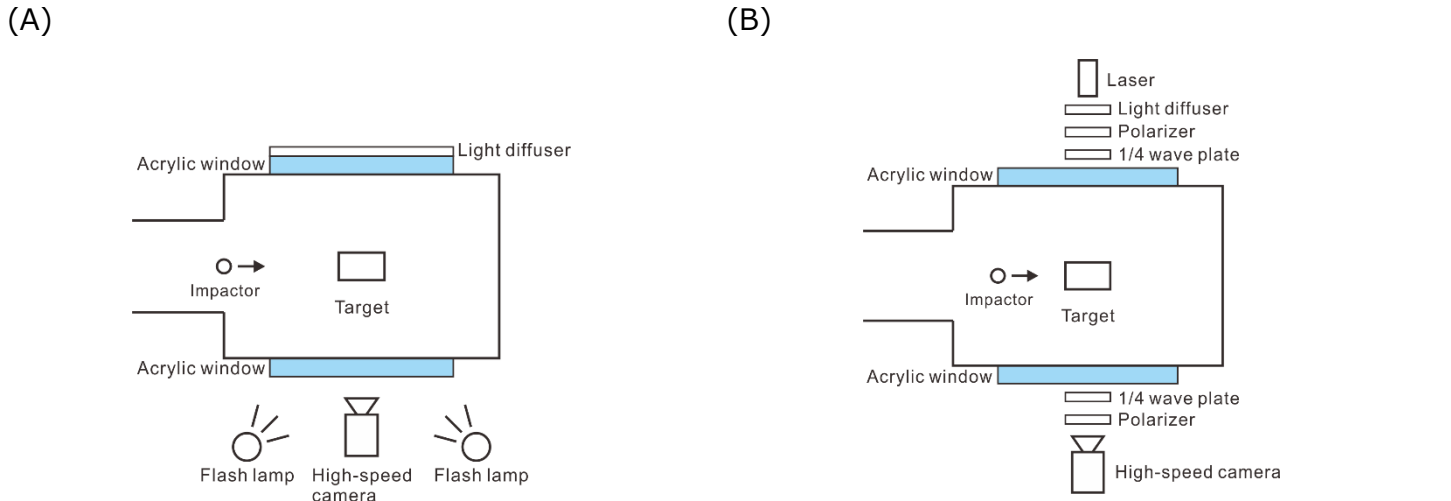
### 1. INTRODUCTION

As the space debris environment worsens with the progress of space development, collisions between spacecraft and space debris are becoming a more serious problem. As a countermeasure against space debris, methods to suppress the generation of new debris and reduce the number of existing debris are being considered, while it is also essential to improve the resistance of spacecraft to space debris collisions. Research on hypervelocity-impact damage of structural materials for spacecraft has been carried out intensively on metallic materials, which are the main structural materials [1-3]. On the other

hand, inorganic materials such as glass and ceramics are increasingly being used as mechanical and structural materials due to the demand for optical and thermal properties associated with the high functionality of spacecraft [4]. However, since such inorganic materials generally fracture brittle, the damage caused by debris impact is more severe than that of ductile metallic materials. The damage mechanism caused by hypervelocity impact is closely related to the process of stress wave propagation and may differ significantly from the quasi-static damage mechanism. Therefore, experimental evaluation of hypervelocity-impact damage in brittle materials is desirable.

In the studies of damage and fracture caused by hypervelocity impact, there have been many experimental and theoretical studies focusing on the evaluation of damage morphology in post-impact targets, such as measurement of crater and debris shapes, construction of damage prediction equations and ballistic limit curves, etc. [5-8]. On the other hand, the evaluation of the propagation behavior of hypervelocity impact damage based on real-time observations has been conducted less frequently than post observations.

In the high-speed impact regime, where impact velocities are ~500 m/s, Strassburger and his coworkers have pioneered the visualization and measurement of impact damage evolution in brittle materials (see Ref. 9 and references therein). Using transparent materials such as glass, single crystal (sapphire), and transparent ceramics (ALON) as targets, they have succeeded in high-speed visualization of damage propagation inside materials. From the obtained images, the propagation velocity of damage front and crack velocity of individual cracks were successfully derived, as well as the time evolution of damage shape. In addition, experiments using laminated glass with a polyurethane layer inside the target also revealed that the crack propagation is delayed by the polyurethane layer. Thus, they have provided many insights into the damage process of brittle materials in the



**FIGURE 1:** SCHEMATICS OF EXPERIMENTAL CONFIGURATION FOR (A) SCATTERED LIGHT IMAGING AND (B) POLARIZED LIGHT SHADOWGRAPH.

high-velocity impact region through visualization of impact events. Real-time measurements of impact events are also desirable in the hypervelocity impact regime, where impact velocities are on the order of km/s, to understand the damage mechanism under hypervelocity impact.

We have investigated the formation and propagation behavior of stress waves and impact damage by high-speed imaging of hypervelocity impact events using the shadowgraph method [10-12]. However, the shadowgraph method has the disadvantage that the damage is captured as a shadowgraph, which provides little information about the damaged structure. In addition, since the visualization of stress waves by the shadowgraph method depends on the second spatial derivative of the refractive index, it is possible to visualize a compressive stress wavefront with a steep change in refractive index, but it is difficult to visualize the propagation process of a rarefaction with a gently changing refractive index or the stress field itself.

In this study, we aim to clarify the impact damage mechanism of inorganic materials by evaluating the relationship between stress wave propagation and damage formation/development through visualization of the damaged structure by high-speed imaging using scattered light from the impacted target and visualization of the stress field change inside the target by high-speed polarized light shadowgraphy.

Quartz glass and soda-lime glass, which are transparent brittle materials, were used as specimens so that the internal damage could be visualized using visible light. Since glass is an amorphous material, the complex effects of grain boundaries on damage propagation can be neglected, making it an ideal

material for obtaining fundamental knowledge of impact damage behavior in brittle materials.

## 2. MATERIALS AND METHODS

Hypervelocity-impact experiments were conducted using a two-stage light gas gun installed at Institute of Space and Astronautical Science (ISAS), Japan Aerospace Exploration Agency (JAXA) [13]. An aluminum alloy (5052) sphere with a diameter of 3.2 mm was used as the impactor. The overall shape of the glass target was a 60 x 60 x 15 mm plate, and the impactor was impacted perpendicular to the 60 x 15 mm surface, which was the side of the plate target. This impact method, called Edge on Impact, is used as a suitable method to visualize stress wave propagation and damage propagation in the direction of impact [9, 14]. In the usual Edge on Impact experiment, a thinner target relative to height and length ( $t/h=0.1$ ) is used and an impactor larger than the impact surface width (target thickness) is impacted to closely resemble a plane-stress state. However, the target geometry used in this study is thicker relative to its height and length ( $t/h=0.25$ ), and the size of the impactor is smaller than the width of the impact surface. The reason for using targets thicker than the impactor diameter is that the variation in impact point is larger than the impactor diameter because the two-stage light-gas gun used has a long free-flight section of about 6 m to separate the sabot used to launch the spherical impactor [13]. Therefore, the stress state and triaxiality in this experiment are different from those in the previous Edge on Impact tests. However, this experimental configuration was adopted to minimize the superposition of damage and stress fields on the

shooting axis as much as possible and to visualize the propagation process of damage and stress fields more clearly.

To investigate the influence of the presence of an interface inside the target on the formation process of impact damage, a target with a structure consisting of two plates of 60 x 30 x 15 mm superimposed on a 60 x 15 mm face in the direction of the ballistic axis was also used in the soda-lime glass experiments.

In the high-speed imaging of the hypervelocity-impact phenomenon, the damaged structure was visualized by the scattered light from the target, and the stress field change inside the target was visualized by the polarized shadowgraph method. Figure 1 shows schematics of experimental configuration for high-speed imaging. In both visualization methods, the impact phenomena were recorded using an ultra-high-speed video camera (HPV-X, Shimadzu Corp.). The camera was set up so that the shooting angle was 90° to the ballistic axis, and the framing interval was set to 500 ns. For scattered light imaging (Fig. 1 (A)), two flash lamps were used for illumination and were arranged to illuminate from the same direction as that of the camera so that the image was captured by scattered light. For polarized shadowgraph imaging (Fig. 1 (B)), a polarizer and a quarter-wave plate were inserted in front of the high-speed camera and the light source, respectively, to visualize the stress field using the photoelastic effect [15, 16]. A pulsed laser (CAVILUX®, Cavitar Ltd.) was used as the light source. The wavelength and pulse width of the laser is 640 nm and 10 ns, respectively. The timing of the laser irradiation was synchronized with the exposure timing of the high-speed camera.

### 3. RESULTS AND DISCUSSION

Figure 2 shows the results of high-speed imaging of the hypervelocity impact of an aluminum alloy sphere on quartz glass and soda-lime glass by scattered light imaging and polarized shadowgraph. Scattered light imaging and polarized shadowgraphy were performed in independent experiments, and impact velocities for each shot are also shown in Figure 2.


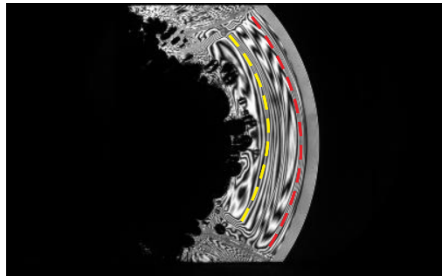
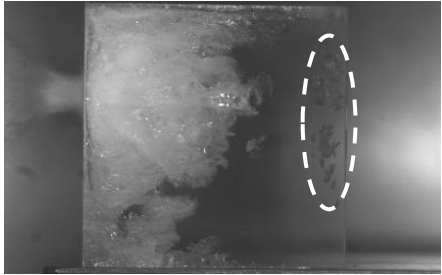
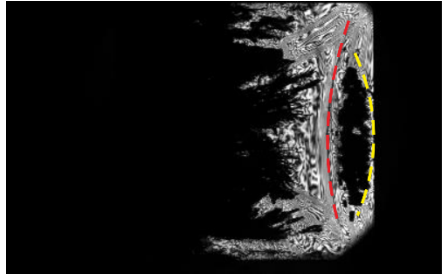
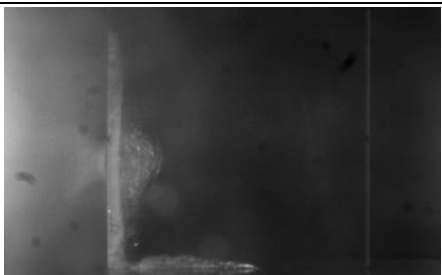
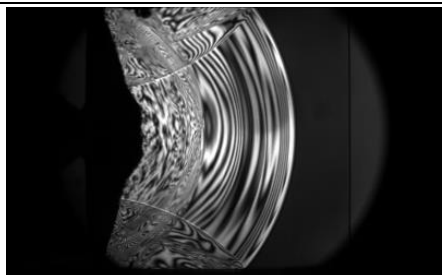

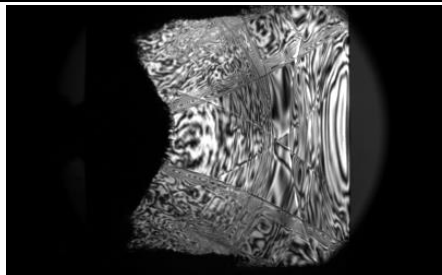
In the scattered light images, the microstructure of the damage formed by the impact is visualized. On the other hand, in the polarized shadowgraph images, the transmitted light intensity depends on the stress birefringence [15, 16], so that the stress field propagated by the impact is visualized. Focusing on the scattered light image, it can be seen that the damage is formed more intensely in quartz glass than in soda-lime glass. The shape of the damage formation is also quite different. In the case of quartz glass, damage propagates from the impact point along the ballistic axis, while in the case of soda-lime glass, damage propagation along the impact surface and the top and bottom surfaces of the specimen is more dominant than damage propagation along the ballistic axis. Differences in damage propagation behavior are also observed between the two types of

glass. In the case of soda-lime glass, the damage propagates continuously from the point of impact, whereas in the case of quartz glass, in addition to the continuous damage from the impact point, isolated damage forms and grows, as can be seen in the area surrounded by the dashed line in the image at 8.0 μs after impact. For quartz glass, it can be seen that the stress wave generated by the impact induces rapid internal damage formation after being reflected by the free surface on the backside, as shown in the area surrounded by the dashed line in the image at 12.5 μs after impact. Such a damage mechanism is similar to the phenomenon called spall fracture [17]. However, the spall fracture surface is usually formed as a flat continuous surface [7, 18], whereas in this experiment, many discontinuous damage points are formed. This difference in the shape of spall damage is thought to reflect the characteristics of quartz glass, which is an amorphous material without grain boundaries that can easily become a crack formation path. However, no damage like this spall fracture is observed in soda-lime glass.

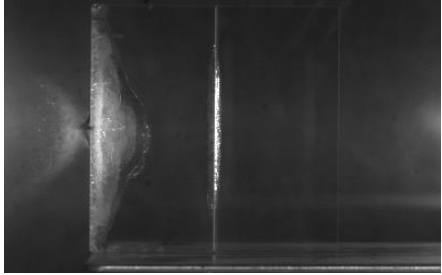

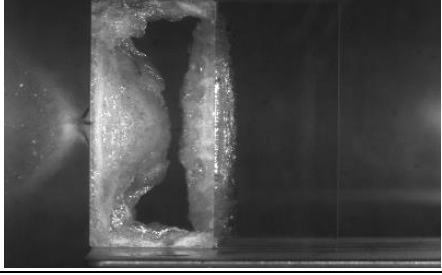
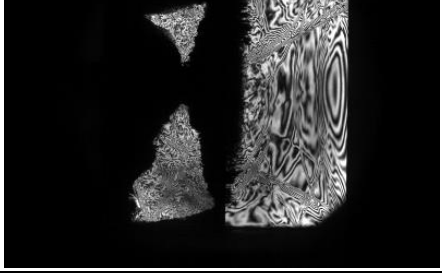
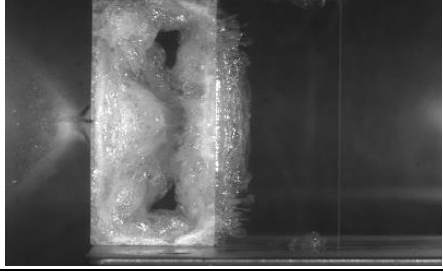
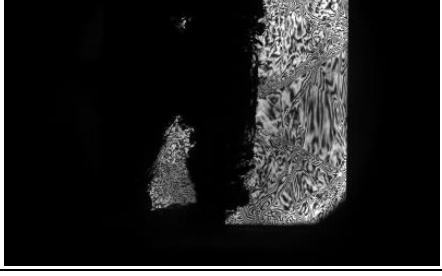
Then, focusing on the images obtained by polarized shadowgraph imaging, there is no significant difference in the structure of the propagating stress field between quartz glass and soda-lime glass. This suggests that the differences in the damage shapes observed between quartz glass and soda-lime glass are due to differences in the damage generation mechanisms of the two materials and the resulting differences in fracture strength. Both materials are amorphous materials consisting of a tetrahedral structure of Si and O atoms, with the only difference being the presence of alkali ions in the tetrahedron of the soda-lime glass [19]. This result shows that such a small difference in structure at the microscopic level has a significant effect on macroscopic impact damage.

The relationship between the propagating stress field and the timing of spall-like damage formation is evaluated by comparing scattered light images and polarized light shadowgraph images for the spall-like damage characteristically observed in quartz glass. In the polarized light shadowgraph images of quartz glass in Figure 2, it is confirmed that spall-like damage is formed at the timing when the stress wave indicated by the red dashed line is reflected at the back surface of the target and interferes with the stress wave indicated by the yellow dashed line that propagates from the impact surface side.

Figure 3 shows time-evolved images of the hypervelocity impact of an aluminum alloy sphere on the target consisting of two blocks of soda-lime glass taken by scattered light imaging and polarized light shadowgraphy. High-speed videography by the scattered light imaging and polarized shadowgraphy were performed in independent impact experiments, and the respective impact velocities are also noted in Figure 3. The contact interface between the blocks is perpendicular to the ballistic axis. As with the single-plate soda-lime glass target

Time after impact	Scattered light imaging	Polarized shadowgraph
	Quartz glass	
	Impact velocity: 3.10 km/s	Impact velocity: 3.15 km/s
at 8.0 $\mu$ s		
at 12.5 $\mu$ s		
	Soda-lime glass	
	Impact velocity: 3.23 km/s	Impact velocity: 3.31 km/s
at 8.0 $\mu$ s		
at 12.5 $\mu$ s		

**FIGURE 2:** TIME EVOLVED IMAGES EXTRACTED FROM HIGH-SPEED VIDEO RECORDINGS OF HYPERVELOCITY IMPACT ON QUARTZ GLASS AND SODA-LIME GLASS TAKEN BY SCATTERED LIGHT IMAGING AND POLARIZED SHADOWGRAPHY. IMPACT VELOCITIES FOR EACH VIDEOGRAPHY ARE ALSO NOTED.

Time after impact	Scattered light imaging	Polarized shadowgraph
	Impact velocity: 3.27 km/s	Impact velocity: 3.19 km/s
at 8.0 $\mu$ s		
at 12.5 $\mu$ s		
at 15.0 $\mu$ s		

**FIGURE 3: TIME EVOLVED IMAGES EXTRACTED FROM HIGH-SPEED VIDEO RECORDINGS OF HYPERVELOCITY IMPACT ON SODA-LIME GLASS MULTIPLE-PLATE TARGETS TAKEN BY SCATTERED LIGHT IMAGING AND POLARIZED SHADOWGRAPHY. IMPACT VELOCITIES FOR EACH VIDEOGRAPHY ARE ALSO NOTED.**

shown in Figure 2, the scattered light image at 8.0  $\mu$ s after impact shows that damage propagation along the impact plane is more dominant than along the ballistic axis. The time evolution of the scattered light images shows that, as in the case of the single-plate target, the damage is formed and propagates along the upper and lower surfaces as the damage near the impact surface develops. In addition, the damage is also formed at the contact interface, and this damage propagates in both the forward and backward blocks. As can be seen from the scattered light and polarized light shadowgraph images at 8.0  $\mu$ s after impact, the damage formed at the interface is independent of the development of damage on the impact surface side, and its formation is triggered after the impact-induced stress waves reach the interface. The results indicate that in brittle materials, the bonding interface functions as a damage formation site due

to the interaction with stress waves and significantly affects the damage formation process. Material composites are one of the most fundamental methods in the development of advanced functionality in modern structural materials. Therefore, it is very important to understand the influence of the presence of bonding interfaces on impact damage formation. It is necessary to focus on the interaction between stress waves and interfaces as one of the mechanisms of impact damage in brittle materials and to evaluate and study the impact damage process.

It has been also suggested that the formation and propagation of hypervelocity impact damage in brittle materials are strongly influenced by the interference between stress waves and damage [11, 20], in addition to the interference between stress waves and the interaction between stress waves and the interface observed in this study. The polarized light

shadowgraphy employed in this study can provide image information on stress field propagation, and is expected to be a very useful measurement tool for evaluating the relationship between the interference morphology of stress waves and damage formation and propagation.

[20] Kimberley, J. and Ramesh, K.T. *Procedia Eng.* **58**, 678 (2013).

#### 4. CONCLUSION

This study demonstrates the usefulness of combining real-time measurements from various imaging methods in the investigation of impact damage mechanisms. This is equally true in comparison with various real-time visualization images obtained from experiments in different impact velocity regimes and experimental geometries. The integrated evaluation and interpretation of damage formation and propagation images under different stress states and triaxialities through numerical simulation is expected to greatly advance the elucidation of the formation process of impact damage and the validation of damage models for impacted materials and is an issue that should be promoted in the future.

#### ACKNOWLEDGEMENTS

This study is supported by ISAS/JAXA as a collaborative program with the Hypervelocity Impact Facility. This work was supported by JSPS Grant-in-Aid for Scientific Research (C) Grant Number JP18K04561 and JP21K04479.

#### REFERENCES

- [1] Cour-Palais, B.G. *Int. J. Impact Eng.* **5**, 221 (1987).
- [2] Cour-Palais, B.G. *Int. J. Impact Eng.* **23**, 137 (1999).
- [3] Christiansen, E.L. and Kerr, J.H. *Int. J. Impact Eng.* **26**, 93 (2001).
- [4] Sawai, S. et al. *Proc. the 56<sup>th</sup> IAC*, IAC-05-C4.3.01 (2005).
- [5] Taylor, E.A. et al. *Int. J. Impact Eng.* **23**, 865 (1999).
- [6] Burt, R.R. and Christiansen, E.L. *Int. J. Impact Eng.* **29**, 153 (2003).
- [7] Kawai, N. et al. *Int. J. Impact Eng.* **38**, 542 (2011).
- [8] Fujiwara, A. et al. *Adv. Space Res.* **54**, 1479 (2014).
- [9] McCauler, J.W. et al. *Exp. Mech.* **53**, 3 (2013).
- [10] Kawai, N. et al. *Procedia Eng.* **58**, 702 (2013).
- [11] Kawai, N. et al. *Procedia Eng.* **103**, 287 (2015).
- [12] Kawai, N. et al. *Procedia Eng.* **204**, 255 (2017).
- [13] Kawai, N. et al. *Rev. Sci. Instrum.* **81**, 115105 (2010).
- [14] Strassburger, E. *Int. J. Appl. Ceram. Tech.* **1**, 235 (2004).
- [15] Lamberson, L. et al. *Exp. Mech.* **52**, 161 (2012).
- [16] Kawai, N. et al. *Int. J. Impact Eng.* **142**, 103584 (2020).
- [17] Shockey, D.A. et al. *J. Appl. Phys.* **46**, 3766 (1975).
- [18] Moritoh, T. et al. *J. Appl. Phys.* **93**, 5983 (2003).
- [19] Alexander, C.S. et al. *Int. J. Impact Eng.* **35**, 1376 (2008).